Assessment of capacity curves for transmission line towers under wind loading

S.S. Banik, H.P. Hong* and Gregory A. Kopp

Department of Civil and Environmental Engineering, University of Western Ontario, Canada N6A 5B9
(Received November 5, 2008, Accepted August 27, 2009)

Abstract. The recommended factored design wind load effects for overhead lattice transmission line towers by codes and standards are evaluated based on the applicable wind load factor, gust response factor and design wind speed. The current factors and design wind speed were developed considering linear elastic responses and selected notional target safety levels. However, information on the nonlinear inelastic responses of such towers under extreme dynamic wind loading, and on the structural capacity curves of the towers in relation to the design capacities, is lacking. The knowledge and assessment of the capacity curve, and its relation to the design strength, is important to evaluate the integrity and reliability of these towers. Such an assessment was performed in the present study, using a nonlinear static pushover (NSP) analysis and incremental dynamic analysis (IDA), both of which are commonly used in earthquake engineering. For the IDA, temporal and spatially varying wind speeds are simulated based on power spectral density and coherence functions. Numerical results show that the structural capacity curves of the tower determined from the NSP analysis depend on the load pattern, and that the curves determined from the nonlinear static pushover analysis are similar to those obtained from IDA.

Keywords: Transmission tower; wind load; nonlinear static pushover analysis; incremental dynamic analysis; capacity curve.

1. Introduction

Overhead power transmission towers are designed and constructed using appropriate design standards such as ASCE Manual No. 74 (1991) and CSA C22.3.1-06 (2006). In particular, the codes recommend the applicable design wind speeds, gust response factors and wind load factors for the design of transmission towers. The gust response factor relates the equivalent static wind load to the overall wind load effects, including both the mean wind and the fluctuating wind load effects. Use of this factor facilitates the design. In addition, the suggested design wind load is calibrated based on the assumption that the tower behaves elastically during a wind event. However, this design approach does not provide any insight into inelastic tower behavior under extreme wind loading, even though the consideration of inelastic response can be important (Lee and McClure 2007). Furthermore, failure of towers under extreme wind loading has been documented in the literature (Li 2000, Savory, *et al.* 2001). Therefore, it is relevant to assess the capacity of the transmission

---

* Corresponding Author, E-mail: hongh@eng.uwo.ca

towers considering both elastic and inelastic responses.

While the assessment of inelastic response under wind loading is not frequently carried out, the inelastic behaviour of structures under extreme seismic loading has been investigated extensively using inelastic static and dynamic analysis methods. A simple nonlinear static method, often employed to characterize structural capacity under seismic load, is known as the nonlinear static pushover (NSP) analysis method (for example, Krawinkler and Seneviratna 1998). As well, the incremental dynamic analysis (IDA) method (Vamvatsikos and Cornell 2002) has become popular in recent years. Both of these methods are used to evaluate the structural capacity curves considering seismic excitations. It should be noted that the differences between earthquake excitations and wind loading include that the former is zero mean random excitations whereas the latter contains significant non-zero mean components and the duration for earthquake excitations compared to that of wind is relatively short (at least for hurricanes and synoptic winds, but not necessarily for tornadoes). Studies focused on the accumulation of permanent set or the damage rate of single-degree-of-freedom (SDOF) systems under wind loading include those of Vickery (1970), Wyatt and May (1971) and Hong (2004). However, the assessment of capacity curves and the evaluation of accumulation of permanent set for transmission line towers under dynamic wind excitations have not been explored.

The objective of this study is to evaluate the capacity curve of a transmission line tower under static and dynamic wind load considering the inelastic structural behaviour. For the evaluation of the structural capacity under wind loading, both the NSP analysis method and the IDA method that are commonly considered in earthquake engineering, are slightly modified and employed in this study. To the authors' knowledge, the use of the former is rarely considered while the use of the latter has not been reported in the literature for wind loading. For the IDA, it is considered that fluctuating wind speeds are characterized by power spectral density functions, while time histories can be simulated using a method developed by Samaras, *et al*. (1985). Comparison of the structural capacity curves developed using the nonlinear static and dynamic analysis methods are also carried out to provide recommendations on the suitable procedures to assess the structural capacity under such wind loading.

2. Evaluation of structural capacity under wind loading

2.1. Use of the nonlinear static pushover procedure

Two often employed methods for evaluating the structural capacity under earthquake loading, the NSP and IDA methods, are adopted in the present study for assessing the capacity of a transmission tower under wind loading.

The NSP analysis method is a popular and routinely used method for seismic performance evaluation of buildings. The method is expected to capture the essential features of the structure that significantly affect its performance. The results can be used to assess the structural capacity or to characterize the load-deformation curve by monotonically increasing the lateral loads with a predefined height-wise lateral load distribution. The method is adequate if the response of a multi-degree-of-freedom system is dominated by its first-mode, since the analysis assumes that the structural vibration mode remains unchanged and independent of its deformed shape. The selection of a height-wise lateral load distribution pattern in the NSP analysis is expected to represent the

distribution of inertial forces in a design earthquake. For seismic loading, the commonly adopted patterns include a rectangular pattern, an inverted triangular pattern and the pattern matched with the first mode deformed shape obtained from a linear elastic dynamic analysis (Krawinkler and Seneviratna 1998).

The NSP analysis is rarely employed for assessing the structural capacity under wind loading. This is perhaps partly due to the fact that the seismic design philosophy allows the structures to undergo a permanent inelastic deformation under severe seismic excitations and the design for wind actions does not take the advantage of the ductile structural capacity. It is noted that an example application of the NSP analysis method for wood frame structures subjected to lateral wind load was presented by Lee and Rosowsky (2006).

If the NSP analysis method is adopted for assessing the capacity of a transmission line tower, the first issue that needs to be considered is the height-wise lateral wind load distribution pattern. In this study, five possible load distribution patterns, namely the rectangular pattern, the inverted triangular pattern, the pattern that matches the first vibration mode shape of the tower, the power law pattern and the pattern resulting from a simulated tornado wind field are considered along with the patterns resulting from design wind load distributions. The load pattern associated with the tornado wind field, which is based on the model given by Twisdale and Dunn (1983), will be discussed further below, in Section 3.2. These five patterns are illustrated in Fig. 1. The first three patterns are those often used for seismic excitations, the fourth one is used to approximate the square of the height-wise boundary layer wind speed variation and the last one is the square of the height-wise horizontal wind speed profile in a simulated tornado whose maximum horizontal wind speed is 160 km/hr with a translation speed of 40 km/hr. This tornado wind load profile is based on the consideration that the tower is approximately located 50 m away from the center of the tornado. Note that, the tornado wind load profile could differ depending on the distance from the center of tornado to the tower and the parameters used in the wind field model. Using one of these considered load distribution patterns, the structural analysis is carried out for monotonically increasing horizontal forces. The results of the analysis are then employed to define the capacity curves in terms of the total horizontal force (or the total reacting base shear force) versus the displacement at the top of the transmission tower. Incipient collapse may be defined by the point where there is non-convergence for an increased lateral load, provided that a stable and reliable numerical method is used for the analysis, or by using the maximum ductility displacement capacity. It is anticipated that such a capacity curve could be approximated by a bilinear inelastic
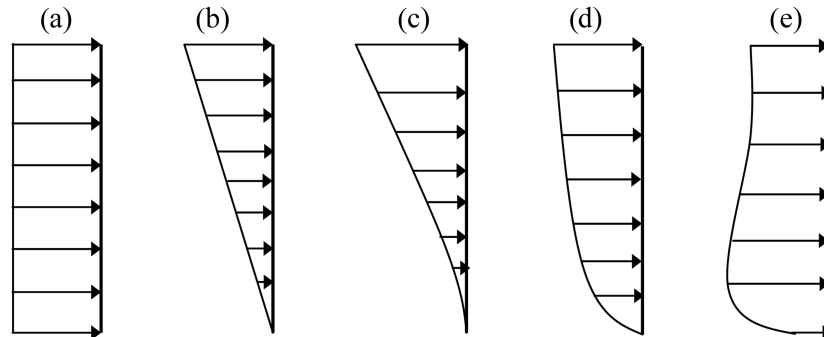

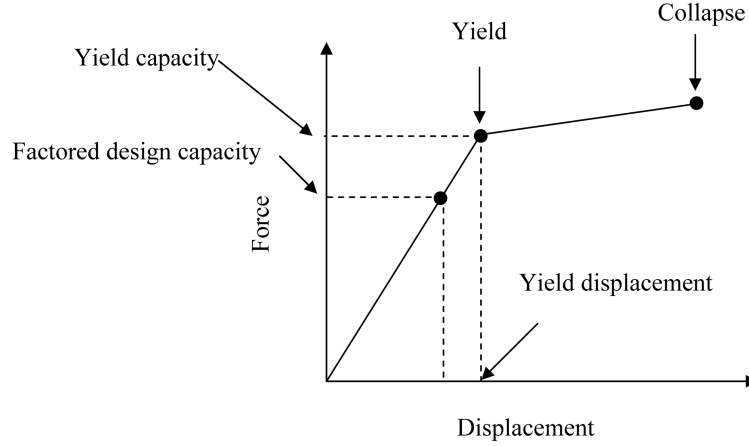Fig. 1 Load patterns. (a) Rectangular, (b) Inverted triangular, (c) First mode, (d) Power law, (e) Tornado

Fig. 2 Force-deformation curve for bilinear elastic system

system, as illustrated in Fig. 2.

According to the CSA C22.3.1-06 (2006), the wind load on an overhead power transmission line tower is distributed based on the calculated wind load acting on its various panels and cables. The wind load is estimated using,

$$F = 0.056\tau V_T^2 CGA,$$ (1)

where F (N) is the total wind load acting on a panel or a cable; τ is the air density correction factor which is usually equal to one for typical design conditions; V_T (km/hr) is the design hourly mean wind speed defined as the T-year return period wind speed; C is the drag coefficient for the exposed face of the panel or the cable; G is the combined wind load factor which is a function of gust response factor, terrain roughness and the height of the center of gravity of each panel or cable; and A is the total surface area of a panel or cable projected normal to the direction of wind. The drag for different panels of a transmission line tower is variable due to the airflow resistance of individual members and airflow patterns around the members of a panel and, therefore, is a function of the solidity ratio (i.e., the ratio of the area of all members in the windward face of the panel to the area of the outline of the windward face of that panel). CSA C22.3.1-06 provides the value of the drag coefficients to be used in the wind load calculation for a transmission tower. For lattice structures having flat-sided members, the value of the drag coefficient accounts for both the windward and leeward faces, including the shielding of the leeward face by the members in the windward face. The combined wind load factor G takes into account the wind speed variation over the height of a tower. Since the loads resulting from Eq. (1) are to be applied to panels, they may not necessarily follow the power law profile discussed previously. More specifically, based on the design recommendations in CSA C22.3.1-06 and ASCE Manual No. 74 (1991), it is assumed that the leeward members of a tower are completely shielded by the windward ones and the total wind load on any panel is placed as a point load on a node on the windward side. This loading scheme will be illustrated below for a tower. In reality, wind load acts on every location on the windward side across the tower height and leeward members are not completely shielded. Therefore, the wind load pattern used for the NSP analysis of a transmission line tower needs to be investigated, which will be discussed shortly.

2.2. Use of incremental dynamic analysis procedure

It should be noted that there are several known drawbacks associated with the NSP analysis (Krawinkler and Seneviratna 1998, Villaverde 2007). These include that the procedure does not have any rigorous theoretical background, and that the procedure is primarily based on the debatable assumptions that the nonlinear response of a structure can be evaluated by an equivalent SDOF structure and that the height-wise loading pattern remains the same during the response history of the structure. The procedure also ignores the duration of the load effects due to cyclic loads and progressive changes in the dynamic properties after yielding.

To overcome some of these drawbacks, the incremental dynamic analysis (IDA) may be employed to characterize the capacity of a transmission tower. The IDA is a numerical procedure used to assess the global behaviour of a structure from its elastic response to global dynamic instability through yielding and nonlinear response (FEMA 2000; Vamvatsikos and Cornell 2002, 2005; Giovenale, *et al.* 2004). The IDA procedure for seismic loading requires a series of linear/nonlinear dynamic analyses to be carried out for a few selected, strong ground motion records that are scaled using an intensity measure. The results are then employed to characterize the capacity curve in terms of the earthquake intensity measure, base shear versus lateral displacement, or drift ratio. Note that although the IDA has only been used for structures under earthquake loading, it could be adopted, with very slight modification, for the evaluation of structural capacity under wind loads.

In order to apply the IDA to structures under wind loading, we note that, unlike seismic loading which consists of zero mean stochastic excitations, the drag force can be represented as the sum of the non-zero mean load due to the mean wind speed and a stochastic excitation due to the fluctuating wind speed. For a two-dimensional structure, this drag force, $F(t, z)$ at time, t, and height, z, can be expressed as,

$$F(t, z) = 0.5\rho CA \overline{V(z)}^2 \left(1 + \frac{v(t, z)}{\overline{V(z)}}\right)^2 = 0.5\rho CA \overline{V(z)}^2 (1 + I(z)\kappa(t, z))^2, \qquad (2)$$

where ρ is the density of air; C is the drag coefficient; A is the area exposed to wind; $\overline{V(z)}$ is the mean wind speed; $v(t, z)$ is the fluctuating component of the wind speed; $I(z)$ is the longitudinal homogeneous turbulence intensity; and $\kappa(t, z)$ is the normalized fluctuating wind speed with zero mean and unit variance. Eq. (2) represents a combination of the mean (i.e., static) drag force and the fluctuating (i.e., dynamic) drag force. Eq. (2) can be used to calculate the total dynamic force acting on the panel or cable of a transmission tower. However, the mean wind speed for a particular site should be adjusted for the height of the panel or the height of the cable since the mean wind speed varies with height. This variation can be described by a logarithmic law or a power law (Simiu and Scanlan 1996). The latter has been widely used in many design codes due to its simplicity. The mean wind speed at a height z above the ground, $\overline{V(z)}$, can be calculated using the following power law function for an open country terrain (Davenport 1965),

$$\overline{V(z)} = \overline{V}_{10} \times (z/10)^{0.16}, \qquad (3)$$

where $\overline{V}_{10}$ is the mean wind speed at 10 m height. In the above expression, it is assumed that the roughness length of the terrain is approximately 0.07 m.

Since the fluctuating wind speed $v(t, z)$ is often assumed to be a Gaussian stochastic process, $\kappa(z, t)$ is also a Gaussian stochastic process and can be characterized by its power spectral density function, $S(f)$, where f (Hz) is the frequency. Throughout this study, $S(f)$ will be represented by the

Kaimal spectrum (Kaimal, *et al*. 1972), but with unit variance,

$$S(f) = \frac{22z/\overline{V(z)}}{(1 + 33fz/\overline{V(z)})^{5/3}}. \tag{4}$$

Davenport's coherence function (Davenport 1968) is adopted for modeling the spatially correlated wind speed. This coherence function is given as,

$$\mathrm{coh}(z_i, z_j, f) = \exp\left[-\frac{fC_z|z_i - z_j|}{\left[\overline{V(z_i)} + \overline{V(z_j)}\right]/2}\right], \tag{5}$$

where C_z is the exponential decay coefficient describing the relative effect of separation in the z direction, while z_i and z_j denote the height of two points.

Based on the above power spectral density function and coherence function, the time history of spatially varying fluctuating wind speed (i.e., wind field), $\kappa(t, z)$, can be simulated using the algorithm given by Samaras, *et al*. (1985), which was based on an auto regressive moving average (ARMA) model. According to the algorithm, the normalized fluctuating wind speeds at any time t can be represented as,

$$\{\kappa(z, t)\} = \sum_{i=1}^{p} [\alpha_i]\{\kappa(z, t - i\Delta t)\} + \sum_{i=0}^{q} [\beta_i]\{\varepsilon_i\}, \tag{6}$$

where $\{\kappa(z, t)\}$ is an *n*-variate vector of normalized fluctuating wind speed at different heights, n denotes the number of points along the height of the tower for which the fluctuating wind speeds are to be generated, $[\alpha_i]$ and $[\beta_i]$ are $n \times n$ autoregressive (AR) and moving average (MA) ARMA coefficients, respectively, for the i-th time step, Δt is the time interval and $\{\varepsilon_i\}$ is the *n*-variate Gaussian white noise series and p and q are the orders of the AR and MA components, respectively. Note that $[\alpha_i]$ and $[\beta_i]$ depend on the mean wind speed $\overline{V(z)}$ since the spectrum for the normalized fluctuating wind speed and the coherence function, shown in Eqs. (4) and (5), are functions of $\overline{V(z)}$. Use of this algorithm to generate fluctuating wind due to downburst was considered by Chay, *et al*. (2006).

Once the mean wind speed and time history of the fluctuating wind speed at desirable locations are known, the IDA of a transmission tower under the time varying wind load in Eq. (2) can be carried out following the steps given below:

1. Calculate the mean wind speed and generate the spatially correlated fluctuating wind speed time histories for different locations of a tower using Eqs. (3)-(6) and Samaras, *et al*. (1985) procedure.
2. Calculate the wind loads acting on different locations of the tower using Eq. (2).
3. Apply the obtained wind loads for a nonlinear structural dynamic analysis using a finite element analysis software package. Note that to avoid a sudden application of the wind load at the start of the analysis, a ramp load that starts from zero and gradually increases to the mean drag load is applied to the structure over the first few seconds. Once the mean drag load is reached, the generated time varying wind loads are then applied.
4. Extract and save the maximum displacement and the maximum base shear forces from the response time history.

5. If the convergence in the structural analysis is observed in Step (3), scale the mean wind speed upwards, and repeat Steps (1) to (4) using the same sequence of $\{\varepsilon_i\}$.

The obtained series of the maximum displacements and the maximum base shear forces provide a sample of the structural capacity curve under dynamic wind loading. It must be emphasized that for a given wind load time history acting on a transmission tower, many of the commercially available structural analysis software packages could be used to carry out the nonlinear dynamic analysis. In this study, a nonlinear direct integration time history analysis method with Hilber-Hughes-Taylor scheme is employed using SAP2000 (Computers and Structures Inc. 2000).

3. Capacity curve of a transmission tower

3.1. Tower description

For the numerical analysis, a 110-KV tangent type lattice steel tower similar in geometry to that described by Natarajan and Shantakumar (1995) is considered. The tower, shown in Fig. 3(a), has a height of 25.25 m with a 3.52 m × 3.52 m square base area. The tower has a total of 316 members and 111 joints. All members of the tower are taken as equal-legged angle sections and are divided into five different groups as shown in Fig. 3(a). The sectional properties of each group are given in
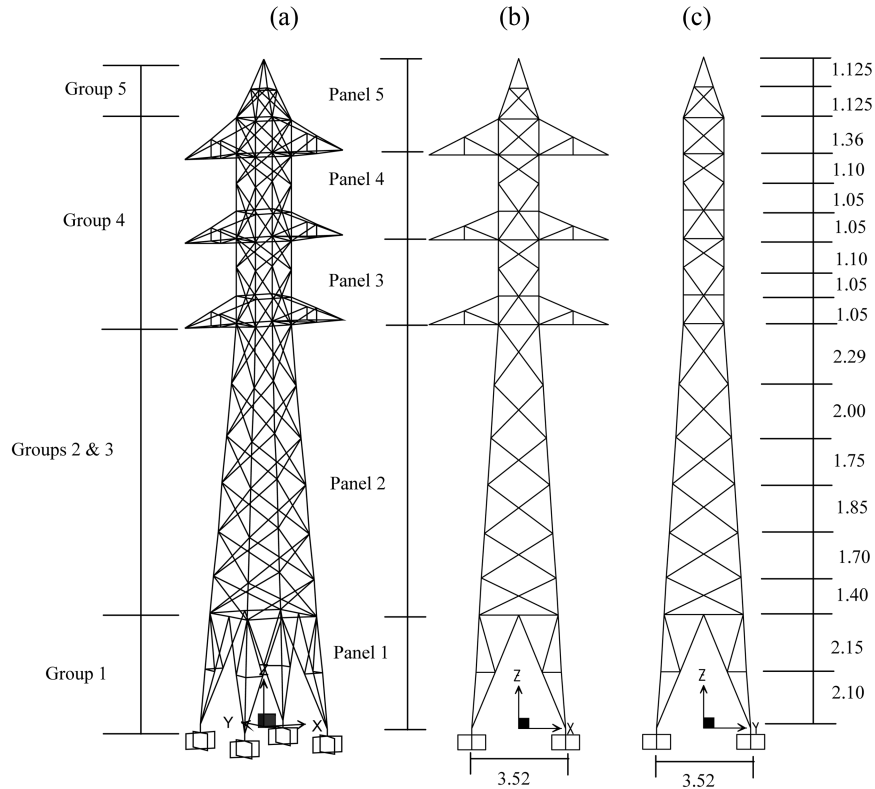

Fig. 3 Example transmission line tower. (a) 3D view, (b) Transverse load carrying face in XZ plane, (c) Longitudinal load carrying face in YZ plane

Table 1 Tower member groups and specification

Group	Member type	Size (mm)
1	Main members and bracings	$125 \times 125 \times 10$
2	Main members	$100 \times 100 \times 10$
3	Bracings	$75 \times 75 \times 6$
4	Main members and bracings	$65 \times 65 \times 8$
5	Main members and bracings	$45 \times 45 \times 5$

Table 2 Conductor and ground wire specification

	Specification	Diameter (m)	Weight (N/m)	Rated strength (N)	Sag (m)
Conductor	95400 cm 45/7 ACSR (RAIL)	0.03	15.9	115209	4.38
Ground wire	3 No. 6 Alumoweld	0.009	2.6	45725	1.83

Table 1. The mean yield strength of the angle sections is 2.48×10^8 (N/m^2). The tower is assumed to be in a transmission line where the span between successive towers is 300 m and the line angle is assumed to be zero. The specifications of the conductors and the ground wire are given in Table 2, which also includes the estimated sags of these components under self weight. A 1.8 m insulator with 75 kg weight is placed between the conductor and the cross arm.

In a linear elastic analysis of lattice steel towers using the finite element method, the members are commonly modeled using truss elements (Da Silva, *et al*. 2005). However, modeling the tower members using frame elements provides better results than those using truss elements when numerical accuracy of nonlinear or inelastic responses are of concern (Lee and McClure 2007). As the present study focuses on the structural behavior of the tower beyond the linear elastic limit, the members of the tower are modeled using frame elements, possible formation of plastic hinges is assigned at the ends of each member to mimic the nonlinear force-deformation relation of the members resulting from the interaction of the axial and flexural stresses and, buckling of individual members is not considered. For the numerical analysis, the default hinge properties implemented in SAP2000, which are based on FEMA-356 (FEMA 2000) criteria, are employed where a post yield stiffness of 3% of the elastic stiffness is allowed for the hinges before collapse and the reduction of plastic modulus due to section slenderness is neglected. Since the actual behavior of lattice tower member connections is close to semi-rigid (Da Silva, *et al*. 2005), the member connections for the example tower are assumed to be rigid, for simplicity. For the numerical analysis to be carried out, the tower is modeled as a two-dimensional frame structure under transverse and longitudinal wind loads in the XZ- and YZ-planes, respectively. These two-dimensional structures, representing the longitudinal and transverse load carrying faces of the tower, are shown in Figs. 3(b)-(c), respectively.

Modal analyses for the considered structure indicate that the first three natural vibration frequencies of the structure shown in Fig. 3(b) are 4.29, 15.38, and 16.34 (Hz), respectively; those of the structure shown in Fig. 3(c) are 5.64, 20.89 and 36.62 (Hz), respectively.

3.2. Capacity curve based on nonlinear static pushover analysis

The tower is divided into five panels (see Fig. 3) and the total static wind load acting on each

panel is to be calculated using Eq. (1) and CSA C22.3.1-06 (2006). Wind loads along the longitudinal direction (i.e. wind load is acting in the direction parallel to the transmission line) and along the transverse direction (i.e. wind load is acting in the direction perpendicular to the transmission line) are considered. For the former, the structural analysis is carried out for the longitudinal load carrying face of the tower in the YZ-plane, whereas for the latter the analysis is carried out for transverse load carrying face of the tower in the XZ-plane. The calculated total longitudinal and transverse loads acting on different panels are shown in Table 3 along with the values of the parameters that are needed for Eq. (2). The calculation was carried out for a reference hourly mean wind speed (at 10 m height) of 100 km/hr. In other words, the calculated wind load does not necessarily represent the actual design wind load, and if the actual design wind speed V_d (e.g., for a 50-year return period) for a site is given, the design wind load is simply equal to those shown in Table 3 multiplied by $(V_d/100)^2$. The transverse wind loads on the conductors and the ground wire, as well as the recommended values of C and G in CSA C22.3.1-06 (2006), are shown in Table 4. This table also includes the vertical loads due to structural dead loads of the conductors and ground wire. The vertical load of the conductor also includes the weight of the insulators. The transverse wind load shown in Table 4 ignores the wind load on the insulators. As mentioned previously, only two-dimensional structural analyses are performed for the structures shown in Figs. 3(b)-(c) under transverse and longitudinal wind loading, respectively. Since these two-dimensional structures represent the longitudinal and transverse load carrying faces of the tower, only one-half of the loads given in Tables 3 and 4 are applied. Since the design codes do not have explicit recommendations about the placement of these loads on the tower for the structural analysis, the

Table 3 Longitudinal and transverse loads on the example tower

	Panel	A (m^2)	Solidity ratio	C	G	F (N)
Longitudinal load	1	3.4	0.25	2.7	1.5	7711
	2	4.98	0.2	2.9	1.9	15366
	3	2.15	0.32	2.42	2.1	6119
	4	2.15	0.32	2.42	2.2	6410
	5	2	0.26	2.6	2.2	6407
Transverse load	1	3.4	0.25	2.7	1.5	7711
	2	4.98	0.2	2.9	1.9	15366
	3	1.38	0.29	2.45	2.1	3976
	4	1.38	0.29	2.45	2.2	4165
	5	3.75	0.3	2.5	2.2	3480

Table 4 Transverse and vertical load on conductors and ground wire

Wire	Transverse load				Vertical load (N)
	Average height (m)	C	G	F (N)	
Conductor 1	11.10	1.00	1.8	8950	5466
Conductor 2	14.30	1.00	1.9	9450	5466
Conductor 3	17.5	1.00	2.0	9950	5466
Ground wire	24.02	1.00	2.1	3130	780

calculated longitudinal and transverse wind loads shown in Tables 3 and 4 are placed on the windward side of the YZ-plane in Fig. 4(a) and the XZ-plane in Fig. 4(b).

In order to find the design capacity of the tower, we note that the load factors for both dead and wind loads can be taken equal to one according to CSA-C22.3 No. 60826 (2006) and AISC-LRFD design code (AISC 1999) for checking the structural steel design. By using these load factors, considering the resistance factors recommended in AISC-LRFD design code (AISC 1999), and carrying out a simple linear static analysis for the loading conditions shown in Figs. 4(a)-(b), it is concluded that the design capacity of the tower is greater than the load effects caused by the hourly mean wind speed of 100km/hr. In fact, by using the structural analysis results, it was found that the considered tower can satisfy the design requirement for the wind speed up to 133 km/hr and 232 km/hr for the XZ- and YZ-planes, respectively. For these design wind speeds, the corresponding base shear forces are 84500 N in the XZ-plane and 113500 N in the YZ-plane.

It must be noted that, as a common practice, the required codified design checking for strength is carried out at structural element level rather than at the structural system level. Since the tower is an indeterminate structural system, the yielding of a structural member may not necessarily lead to the failure of the tower due to load re-distribution and system redundancy. To determine the structural system capacity curve, and to assess the impact of the load distributions on the curve, five static load patterns based on the design load scenarios are considered for the NSP analysis, as listed in Table 5. In the table, the load patterns 1 and 2 (from Tables 3 and 4) are referred to as concentrated
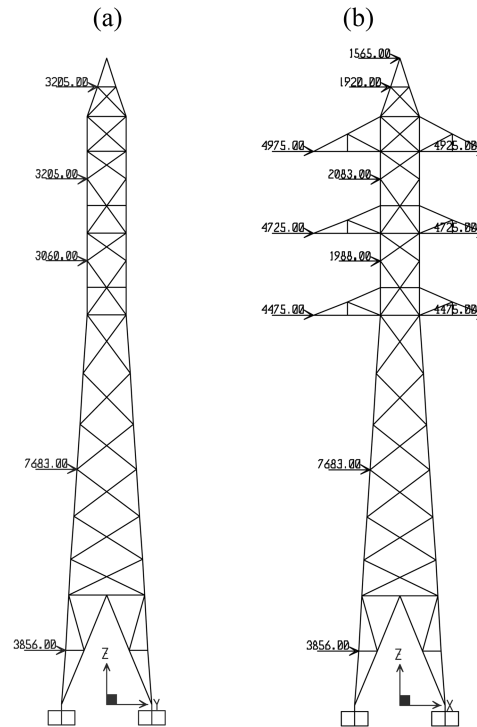

Fig. 4 Static wind load. (a) Longitudinal concentrated wind load pattern on the windward side of the face of the tower in YZ plane, (b) Transverse concentrated wind load pattern on the windward side of the face of the tower in XZ plane

Table 5 Load patterns for NSP analysis

Pattern	Description
1	Longitudinal concentrated loads on windward side of the face of the tower in YZ plane.
2	Transverse concentrated loads on windward side of face of the tower in XZ plane.
3	Longitudinal concentrated loads divided between the windward and leeward side of the face of the tower in YZ plane. according to 2:1 ratio
4	Transverse concentrated loads divided between the windward and leeward side of the face of the tower in XZ plane according to 2:1 ratio
5	Longitudinal wind loads distributed on the windward side of face of the tower in YZ plane.

wind load patterns. These load patterns (i.e., Patterns 1 and 2) correspond to those shown in Figs. 4(a) and 4(b), respectively. For these load patterns, it is considered that the wind load could simply be placed on the windward side on the nodes that are close to the centroids of the respective panels. Additionally, Patterns 3 and 4 are considered to investigate the effect on the structural capacity by placing loads on the windward and leeward sides. The selected ratio of the wind loads on the windward and leeward sides is based on the study given by Savory, *et al.* (2001). Pattern 5 is considered in order to assess the impact of using a wind load distribution caused by the variation of wind speed along the height of the tower on the capacity curve.

For the NSP analysis, SAP2000 is employed and the analysis is carried out for each load pattern depicted in Table 5. More specifically, for each load case, the vertical loads (i.e. structural dead loads) are applied to the structure first. Subsequently, the NSP analysis is carried out by considering the initial condition equal to the stressed condition due to vertical loads, and by applying the horizontal loads according to each load pattern described in Table 5. Note that for the NSP analysis, the horizontal loads are increased monotonically until a desired displacement is reached or a failure (or non-convergence) is observed. Geometric nonlinearity (such as P-Δ effects), which can be significant, is not included in the analysis. This is partly due to the instability of the adopted structural analysis software in dealing with highly nonlinear inelastic responses.

Fig. 5 summarizes the results obtained from NSP analyses for the five load patterns shown in Table 5. The vertical axis of the figure represents the total base shear force (i.e., total horizontal reacting force) for the along wind direction while the horizontal axis represents the displacement at the top of the tower in the same direction. The results shown in Fig. 5 suggest that:

1) In all considered load patterns, there is a clearly identifiable yield point for the tower system. The capacity curves shown in the figure seem to represent bilinear systems.
2) The capacity at yield for the tower in the XZ-plane is significantly lower than that for the tower in the YZ-plane. This is expected since, for the former, a large amount of load resulted from the wind acting on the cables and ground wire is placed on the cross arms and on the top of the tower.
3) Splitting wind loads between windward and leeward sides of the tower (i.e., Patterns 3 and 4) results in slightly higher global capacity at yield than that obtained by placing the wind load on the windward side alone (i.e., Patterns 1 and 2).
4) Placing the total load in a few nodes rather than distributing it to the panels (Pattern 5) results in a lower capacity at yield. This is probably due to the fact that, the load sharing and redistribution of the wind loads are more likely to occur if the loads are originally distributed over the height of the tower.
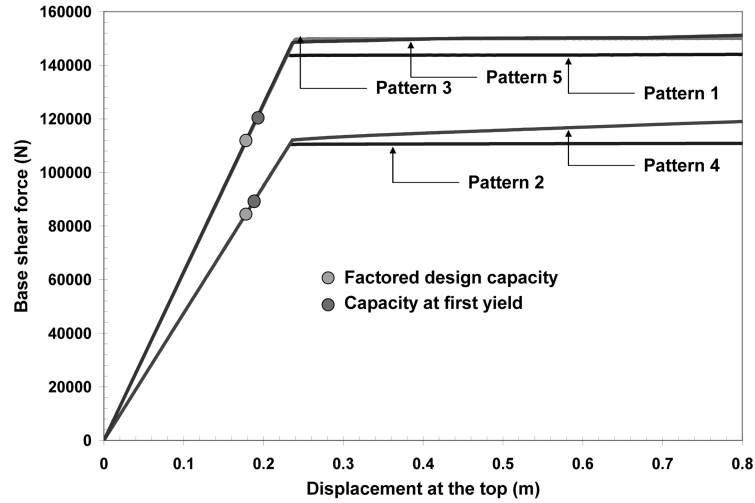
Fig. 5 Capacity curves obtained for different static load cases using NSP

For all the cases shown in Fig. 5, the yielding of the tower starts when the top displacement is about 0.24 m. This corresponds to a drift ratio of approximately 1%.

Note that for Patterns 1 and 2, the first yielding of a member, which refers to formation of the first plastic hinge in the structure, is also identified in Fig. 5. It can be observed that the base shear force corresponding to the first yielding is about 120000 N and 88000 N for the load Patterns 1 and 2, respectively. The capacities at the first yield are about 1.05 times the (factored) design capacities for the design wind speed of 133 km/hr and 232 km/hr mentioned earlier. It must be emphasized that the yield capacity of the tower differs from that identified at the first yield. The former for Pattern 1 and Pattern 2, shown in Fig. 4 are about 143600 N and 110000 N, which are approximately equal to 1.3 times the (factored) design capacity. Fig. 6(a) illustrates the formation of plastic hinges in the structure with increasing lateral load under several steps of the NSP analysis for load Pattern 2. The points in the capacity curve corresponding to these steps are identified in Fig. 6(b). The figure shows the redistribution of the loads after several hinges have been formed.

As stated previously, the NSP analysis method is an approximate method so that the results may be influenced by the adopted load pattern. The load cases considered previously, to a degree, follow the wind load pattern suggested by the design code. If the capacity curve resulting from the use of one of the load patterns shown in Figs. 1(a)-(d) does not differ significantly from the one resulting from the load pattern obtained using code recommendations, then one can avoid the need to evaluate the codified wind load on the transmission line tower for obtaining capacity curve under such load. To investigate whether this is indeed the case, the NSP analyses are carried out for the longitudinal load carrying face of the tower shown in Fig. 3(c) using the loading patterns shown in Figs. 1(a)-(d). Note that in the analysis, the loads resulting from each pattern are applied to the windward side of the YZ-plane. An NSP analysis is also carried out for the pattern shown in Fig. 1(e), which resulted from the height-wise horizontal wind speed variation in a sample tornado. The wind loads following this pattern are calculated at the locations shown in Fig. 4(a) using Eq. (1) and the values of A and C listed in Table 3. Note that the value of G in Eq. (1) is assumed equal to one for all locations while the wind speeds are calculated for an F1 tornado with maximum wind speed of 160 km/hr at 10 m height and about 50 m from its center using a tornado wind field model

(a)

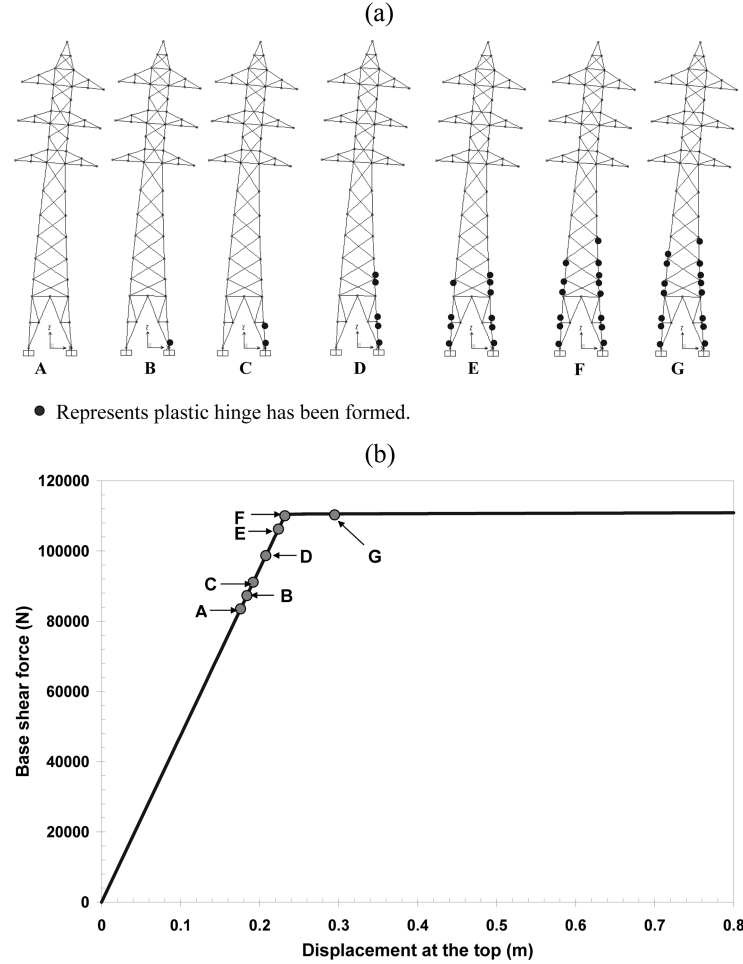● Represents plastic hinge has been formed.

(b)

Fig. 6 Load-deformation characteristics for load Pattern 2. (a) Formation of plastic hinges at different stages of NSP, (b) Capacity curve

(Twisdale and Dunn 1983). The considered parameters for this wind field model are given in the Appendix. The obtained capacity curves from these NSP analyses are plotted as the total base shear force versus the lateral displacement at the top of the tower and are shown in Fig. 7. For comparison purposes, the capacity curve obtained for Pattern 1, depicted in Fig. 4, is re-plotted in Fig. 7. The results shown in the figure indicate that yield points correspond to a drift ratio of about 1%, and that the yield capacity of the tower is sensitive to the adopted load pattern. The sensitivity of the yield capacity to the adopted load patterns in Figs. 1(a)-(e) is further illustrated in Table 6 and compared with the design capacity of the tower in YZ-plane. It is noted from the table that the yield capacity resulting from Pattern 1 is the highest among all the considered load patterns, while the pattern matched with first mode results in lowest yield capacity. The ratio between the estimated yield capacity to the (factored) design capacity ranges from 0.74 to 1.27. However, it must be emphasized that the pattern associated with the inverted triangle and first mode may be unrealistic for the type of wind loading considered in this study. The structural capacity of the tower resulting
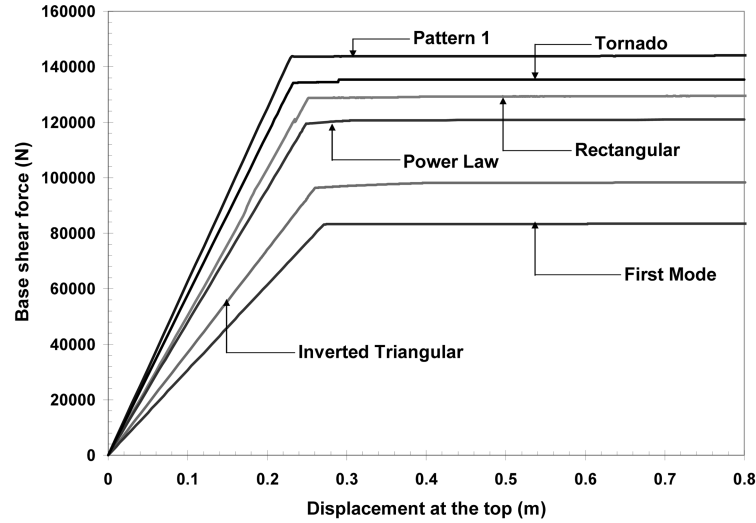
Fig. 7 Capacity curves obtained using NSP analysis for different longitudinal wind load pattern on the windward side of the face of the tower in YZ plane

Table 6 Comparison of yield capacity for different load patterns

Load pattern	Yield capacity	Yield capacity/Design capacity
Pattern 1	143600	1.27
Rectangular	128700	1.14
Inverted triangular	96400	0.85
First mode	83200	0.74
Power law	119500	1.06
Tornado	135500	1.19

from the sample tornado load pattern is slightly lower than that obtained using Pattern 1. Note that the height wise wind profile in a tornado may not be the same shape as presented in Fig. 1e for all of the radial locations due to the variability of wind speeds in a tornado and the height of the structure could impact the estimated capacity curve resulting from the tornado wind load.

One may scrutinize the identified yield capacity at or near system yielding, since second order (i.e., P-Δ) effects are neglected in this analysis. A verification study was performed to assess the P-Δ effects on the system yield capacity. It is observed that for the considered transmission tower the difference between the system yield capacity, including or excluding the P-Δ effects, is less than 3%. It should be noted that the results obtained by including the P-Δ effects, are difficult to obtain after the system yields. This is likely due to the fact that the load-control procedure is adopted for the analysis.

3.3. Capacity curve based incremental dynamic analysis

The incremental dynamic analysis is only carried out for the face of the tower in the YZ–plane, as shown in Fig. 3(c). To carry out the analysis, temporally- and spatially-varying wind loads are

simulated, considering Eq. (2) with the load application locations shown in Fig. 4(a). For the simulation, a reference hourly mean design wind speed (at 10m height) of 100 km/hr is considered and the mean wind speed along the height of the tower is calculated using Eq. (3) accordingly. The normalized, fluctuating, spatially correlated wind speed $\kappa(z,t)$ is simulated by using the algorithm shown in Eq. (6) and by adopting the following assumptions: (i) The value of the decay coefficient C_z is taken as 10 (Simiu and Scanlan 1996), (ii) the streamwise wind turbulence intensity is 16%, (iii) equal orders of the AR and MA components (i.e., $p = 5$ and $q = 5$) are used, and (iv) $\Delta t = 0.05$ sec. To check the validity of the assumptions (iii) and (iv) in producing the fluctuating wind speed defined by the power spectral density function shown in Eq. (4), a verification study was performed in which a series of simultaneous time histories are generated for the load point locations shown in Fig. 4(a). It was observed that in all occasions the spectra and the cross-spectra of the generated time histories match the target spectra. It was observed that the choice of the time interval and the orders of AR and MA coefficients are satisfactory up to 10 Hz for the turbulence. Since the structures shown in Figs. 3(b)-(c) have natural frequencies within that range, no reduction of the time interval is necessary.

Using the simulated temporally- and spatially-varying wind load, the incremental dynamic analysis was carried out in SAP2000. For the analysis, mass and stiffness proportional damping, with 3% of the critical damping ratio, was used. The lumped mass of the conductor and insulator at the end of each cross-arm, and that of the ground wire at the top of the tower, are neglected in the analysis.

Nine IDA curves (i.e., capacity curves derived from IDA results), each with one minute wind load time history for each considered loading level, are generated using the procedure described in Section 2.2. The curves are plotted in Fig. 8 using the maximum displacement and base shear force obtained in each analysis. Fig. 8 also includes the NSP curve obtained for load Pattern 1 for comparison. It is apparent from Fig. 8 that the capacity curves resulting from IDA do not differ significantly from those obtained from NSP and that the variations in the inelastic region are much less than those observed for frame structures designed according to the Canadian standard and subjected earthquake loading (Wang 2006). The latter can be explained by noting that the wind loading is considered herein as a stationary process while earthquake excitations are highly nonstationary.
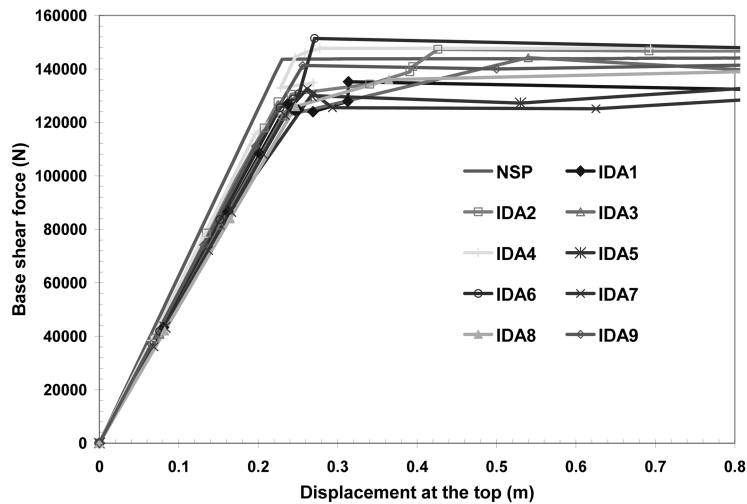

Fig. 8 Capacity curves obtained using IDA for the longitudinal wind load on the windward side the face of the tower in YZ plane

The average curve resulting from the IDA curves is calculated and plotted in Fig. 9 and compared to the NSP curve obtained for load Pattern 1. The figures indicate that the capacity obtained by the NSP is slightly higher than that obtained from the IDA curves. In both cases, the post yield stiffness is low and negligible.

It must be emphasized that the presented incremental dynamic analysis results are carried out using the one minute wind load time history and, cyclic degradation is not considered in the model. To investigate the effects of load duration on the IDA results, an IDA curve for the face of the tower in the YZ-plane is calculated using a five-minute wind load time history. The obtained curve is depicted in Fig. 10 and compared with the one obtained based on one-minute. This comparison
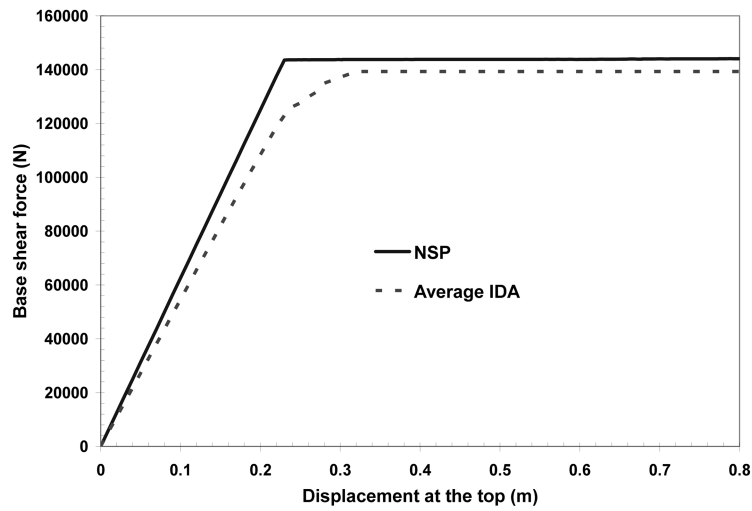

Fig. 9 Comparison of NSP analysis and IDA for the longitudinal wind load on the windward side of the face of the tower in YZ plane
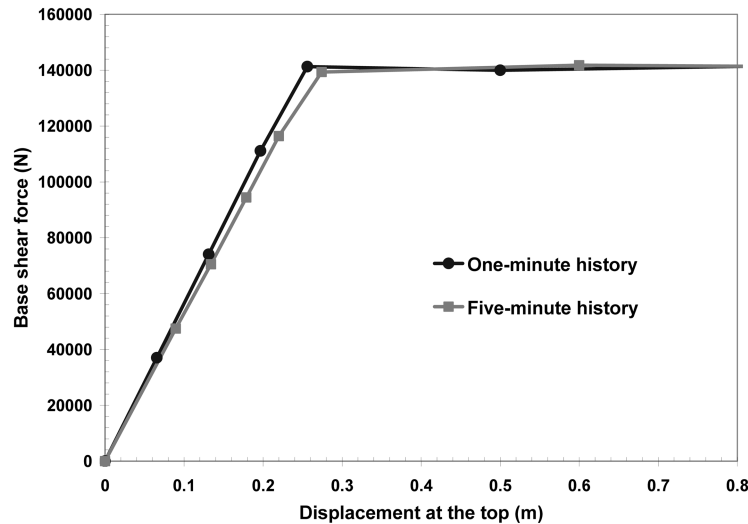

Fig. 10 Comparison of IDA results for different durations of wind loading

indicates that the duration of wind load has little or no effect on the expected IDA curve.

It must be emphasized that the intensity of one-minute and five-minute wind load time histories differ for a given base shear level or top displacement level. The observations drawn from Figs. 7 to 9 simply indicate that the NSP analysis results could be used to provide sufficiently adequate characterization of the capacity of the transmission tower.

4. Conclusions

The study presented in the paper was aimed to characterize the capacity curve of a transmission line tower considering inelastic behaviour under wind loads. Consideration of inelastic capacity in the design procedure for synoptic wind loading may be argued since accumulation of plastic damage over a long period of time may eventually lead to collapse of the structure. However, for short duration high intensity (i.e., comparable to that of earthquake loading) extreme winds, such as tornadoes or downbursts, consideration of ductile behaviour in the design could result in economic design while ensuring the structural safety. It is acknowledged that the results presented in this study may not be considered definitive since the actual probabilistic characterizations of the high intensity tornado and downburst winds are not entirely clear in the wind engineering community. However, the results do imply that the overall structural strength at yield is much higher than the design capacity and that one could take advantage of this difference, and the structural ductility capacity, for designing and assessing reliability of towers under short duration, high intensity wind loading. The results also show that the synoptic wind load profile may lead to overestimation of the load effects when used to characterize the structural capacity of the tower under short duration tornado wind loading.

The conclusions that can be drawn from the numerical results are:

1. The estimated structural capacity of the tower is dependent on the adopted load pattern for the analysis and it is observed that the capacity curves obtained using the load patterns commonly used in earthquake engineering differ significantly from those obtained using the load patterns resulting from the design wind load distribution. It is also observed that use of a tornado load pattern could result in slightly lower capacity. However, this conclusion needs to be further verified considering the variability of wind profiles arising from tornados of different Fujita scales and considering different distances from the center of tornado to the tower.

2. The capacity curves of a transmission line tower obtained from the NSP and from the IDA are similar. The duration of the dynamic wind load used for the IDA has little or no effect on the capacity curve. In arriving at this observation, fatigue and degradation due to cyclic loading are neglected.

3. It is observed that the global capacities of the tower are about 30% higher than the factored design capacity of the structure. This information could be valuable in assessing the capacity of the tower system.

Acknowledgements

References

AISC (1999), *Manual of steel construction: Load and resistance factor design*, American Institute of Steel Construction.

ASCE (1991), *Guidelines for electrical transmission line structural loading*, ASCE manuals and reports on engineering practice No. 74.

Banik, S.S., Hong, H.P. and Kopp, G.A. (2007), "Tornado Hazard Assessment for Southern Ontario", *Can. J. Civil Eng.*, **34**, 809-842.

Chay, M.T., Albermani, F. and Wilson, R. (2006), "Numerical and analytical simulation of downbursts for investigating dynamic response of structures in the time domain", *Eng. Struct.*, **28**(2), 240-254.

Computers and Structures, Inc. (2000), *Integrated structural analysis and design software*, SAP2000 version 7.4. Berkeley, CA.

CSA (2006), *Overhead systems, CSA C22.3.1-06*, Canadian Standards Association, Toronto, Ontario.

CSA (2006), *Design criteria for overhead transmission lines*, *CSA C22.3 No.606828*, Canadian Standards Association, Toronto, Ontario.

Da Silva, J.G.S., Da S. Vellasco, P.C.G., De Andrade, S.A.L. and De Oliviera, M.I.R. (2005), "Structural assessment of current steel design models for transmission and telecommunication towers", *J. Constr. Steel Res.*, **61**, 1108-1134.

Davenport, A.G. (1965), "The relationship of wind structure to wind loading", *Proc. of the Symp. on Wind Effects on Buildings and Structures*, 1. National Physical Laboratory, Teddington, U.K.

Davenport, A.G. (1968), "The dependence of wind load upon meteorological parameters", *Proc. of the Int. Research Seminar on Wind Effects on Buildings and Structures*, University of Toronto Press, Toronto.

FEMA (2000), *Prestandard and commentary for the seismic rehabilitation of buildings*, Publication no. 356, prepared by the American Society of Civil Engineers for the Federal Emergency Management Agency, Washington, D.C.

Giovenale, P., Cornell, C.A. and Esteva, L. (2004), "Comparing the adequacy of alternative ground motion intensity measures for the estimation of structural responses", *Earthq. Eng. Struct. D.,* **33**(8), 951-979.

Hong, H.P. (2004), "Accumulation of wind induced damage on bilinear SDOF systems", *Wind Struct.*, **7**(3), 145-158.

Kaimal, J.C., Wyngaard, J.C., Izumi, Y. and Cote, O.R. (1972), "Spectral characteristics of surface layer turbulence", *Q. J. Roy. Meteorol. Soc.*, **98**, 563-589.

Krawinkler, H. and Seneviratna, G.D.P.K. (1998), "Pros and Cons of a pushover analysis of seismic performance evaluation", *Eng. Struct.*, **20**(4-6), 452-464.

Lee, K.H. and Rosowsky, D.V. (2006), "Fragility curves for wood frame structures subjected to lateral wind load", *Wind Struct.*, **9**(3), 217-230.

Lee, P.S. and McClure, G. (2007), "Elastoplastic large deformation analysis of a lattice steel tower structure and comparison with full-scale tests", *J. Constr. Steel Res.*, **63**, 709-717.

Li, C.Q. (2000), "A stochastic model of severe thunderstorms for transmission line design", *Probab. Eng. Mech.*, **15**, 359-364.

Natarajan, K. and Santhakumar, A.R. (1995), "Reliability based optimization of transmission line towers", *Comput. Struct.*, **55**(3), 387-403.

Samaras, E., Shinozuka, M. and Tsurui, A. (1985), "ARMA representation of random processes", *J. Eng. Mech.* ASCE, **111**(3), 449-461.

Savory, E., Parke, G., Zeinoddini, M., Toy, N. and Disney, P. (2001), "Modeling of tornado and microburst-induced wind loading and failure of a lattice transmission tower", *Eng. Struct.*, **23**, 365-375.

Simiu, E. and Scanlan, R.H. (1996), *Wind effects on structures*, John Wiley & Sons, Inc. New York.

Twisdale, L.A. and Dunn, W.L. (1983), "Probabilistic analysis of tornado wind risks", *J. Struct. Eng.* ASCE, **109**, 468-488.

Vamvatsikos, D. and Cornell, C.A. (2002), "Incremental dynamic analysis", *Earthq. Eng. Struct. D.*, **31**(3), 491-514.

Vamvatsikos, D. and Cornell, C.A. (2005), "Direct estimation of seismic demand and capacity of multi-degree-of-freedom systems through incremental dynamic analysis of single-degree-of-freedom approximation", *J.*

Struct. Eng., **131**(4), 3-19.

Vickery, B.J. (1970), "Wind action on simple yielding structures", *J. Eng. Mech. D.* ASCE, **4**, 107-120.

Villaverde, R. (2007), "Methods to assess the seismic collapse capacity of building structures: state of the art", *J. Struct. Eng*. ASCE, **133**(1), 57-66.

Wang, W. (2006), *Probabilistic assessment of steel frames designed according to NBCC seismic provisions*, PhD Thesis, The University of Western Ontario.

Wyatt, T.A. and May, H. (1971), "Ultimate load behavior of structures under wind loading", *Proc. of the 3rd Int. Conf. on Wind Effects on Buildings and Structures*, Tokyo, Japan.

CC

S.S. Banik, H.P. Hong and Gregory A. Kopp

Appendix. Parameters adopted to generate the tornado wind profile.

Table A1. Value of the parameters employed to generate the wind profile shown in Fig. 1(e) by using the tornado wind field model developed by Twisdale and Dunn (1983).

Parameters	Value
Wind field path width fitting parameter, a	0.09267
Wind field path width fitting parameter, b	99.6256
Boundary layer thickness at the radius of the maximum tangential speed	122 m
Maximum boundary layer thickness	152 m
Core slope	0
Maximum wind speed	160 km/hr
Location of the center of transmission tower from the center of the tornado	50 m
Radius of maximum tangential speed	50 m
Reference height of the maximum wind	10 m
Translation speed	40 km/hr
Parameter for evaluating wind field, α	10
The ratio of the radial to tangential velocity components, γ	0.45
Effective sub layer thickness, ζ	20

Symbols used in this appendix are the same as those used in Twisdale and Dunn (1983).